Electronic Supplementary Information

Infrared spectra and anharmonic coupling of proton-bound nitrogen dimers N_2-H^+-N_2, N_2-D^+-N_2, and $^{15}N_2$-H^+-$^{15}N_2$ in solid *para*-hydrogen

Hsin-Yi Liao,*[a] Masashi Tsuge,*[b] Jake A. Tan,[c] Jer-Lai Kuo[c] and Yuan-Pern Lee[bc]

[a] *Department of Science Education, National Taipei University of Education, 134, Section 2, Heping East Road, Daan District, Taipei 10659, Taiwan*
E-mail: hyliao@tea.ntue.edu.tw; Tel: +886-2-27321104ext.53310
[b] *Department of Applied Chemistry and Institute of Molecular Science, National Chiao Tung University, 1001 Ta-Hsueh Road, Hsinchu 30010, Taiwan*
E-mail: (M.T.) tsuge@nctu.edu.tw; Tel: +886-3-5131459
[c] *Institute of Atomic and Molecular Sciences, Academia Sinica, Taipei 10617, Taiwan*

Table of Contents

A. Comparison of bond lengths, harmonic vibrational wavenumbers, and IR intensities of $(N_2)_2H^+$ at varied levels of theory

The geometry of N_2-H^+-N_2 was optimized at the B3LYP, MP2, and CCSD levels with the aug-cc-pVXZ (X = D, T, and Q, designated as AXZ in Table S1) basis sets. The optimized geometric parameters are presented in Table S1. Optimizations at both MP2 and B3LYP methods resulted in a centrosymmetric linear equilibrium structure with $D_{\infty h}$ symmetry, designated N_2-H^+-N_2. However, the CCSD method gives a centrosymmetric saddle point. As one can see in Table S1, the MP2 and CCSD methods give similar bond lengths for the N-H^+-N structure. B3LYP results show a longer d(H^+–N) and a shorter d(N≡N) when compared with the structures optimized with MP2 or CCSD using the same basis set. The B3LYP method underestimates the interaction between proton and nitrogen molecules and might be unsuitable for the present study.

The NH^+N antisymmetric stretching (ν_4) mode has the largest intensity among ten normal modes of N_2-H^+-N_2. The harmonic vibrational wavenumber of the NH^+N antisymmetric stretch is greater than that of the N_2…N_2 stretching (ν_2) mode, except those calculated with the MP2/aug-cc-pVQZ method. Further, the MP2 method predicts slightly smaller harmonic vibrational wavenumbers than the CCSD method. As the basis set becomes larger, wavenumbers calculated with the MP2 method approach those calculated with the CCSD/aug-cc-pVDZ method. Linnartz *et al.* reported that the MP2 method tends to overestimate the electron-correlation effects when calculating the dissociation energy of N_2-H^+-N_2.[9] Thus, for a better DVR estimation, the CCSD/aug-cc-pVDZ method is chosen to be the appropriate level of theory to perform the structure optimization and calculations of harmonic vibrational wavenumbers.

Table S1 Bond lengths (in Å), harmonic vibrational wavenumbers (in cm^{-1}), and IR intensities (in km mol^{-1}; shown in parentheses) of centrosymmetric linear N_2-H^+-N_2 calculated with varied methods.

	B3LYP			MP2			CCSD	
	ADZ [a]	ATZ [a]	AQZ [a]	ADZ [a]	ATZ [a]	AQZ [a]	ADZ [a]	ATZ [a]
d(H^+–N)	1.285	1.283	1.283	1.280	1.274	1.275	1.281	1.275
d(N…N)	2.569	2.566	2.566	2.560	2.548	2.549	2.562	2.549
d(N≡N)	1.100	1.088	1.087	1.128	1.111	1.108	1.110	1.093
ν_1	2508 (0)	2511 (0)	2510 (0)	2217 (0)	2247 (0)	2261 (0)	2458 (0)	2486 (0)
ν_2	428 (0)	429 (0)	428 (0)	433 (0)	438 (0)	436 (2)	437 (0)	442 (0)
ν_3	2479 (301)	2480 (280)	2480 (279)	2183 (255)	2212 (241)	2226 (237)	2424 (264)	2451 (253)
ν_4	700 (4959)	569 (4953)	544 (4945)	590 (5211)	491 (5171)	430 (5150)	126*i* (5524)	391*i* (5459)
ν_5 [b]	236 (0)	263 (0)	257 (0)	236 (0)	258 (0)	255 (0)	250 (0)	275 (0)
ν_6 [b]	1191 (92)	1214 (91)	1195 (91)	1192 (90)	1227 (86)	1203 (86)	1217 (90)	1256 (89)
ν_7 [b]	135 (5)	141 (6)	137 (6)	132 (6)	139 (7)	135 (8)	141 (6)	148 (7)

[a] ADZ, ATZ, and AQZ denote aug-cc-pVDZ, aug-cc-pVTZ, and aug-cc-pVQZ, respectively. We follow the mode numbering by Duncan and coworkers.[10]

[b] Doubly degenerated vibrational modes.

B. Displacement vectors for normal modes of $(N_2)_2H^+$, $(N_2)_3H^+$, and Ar-$(N_2)_2H^+$

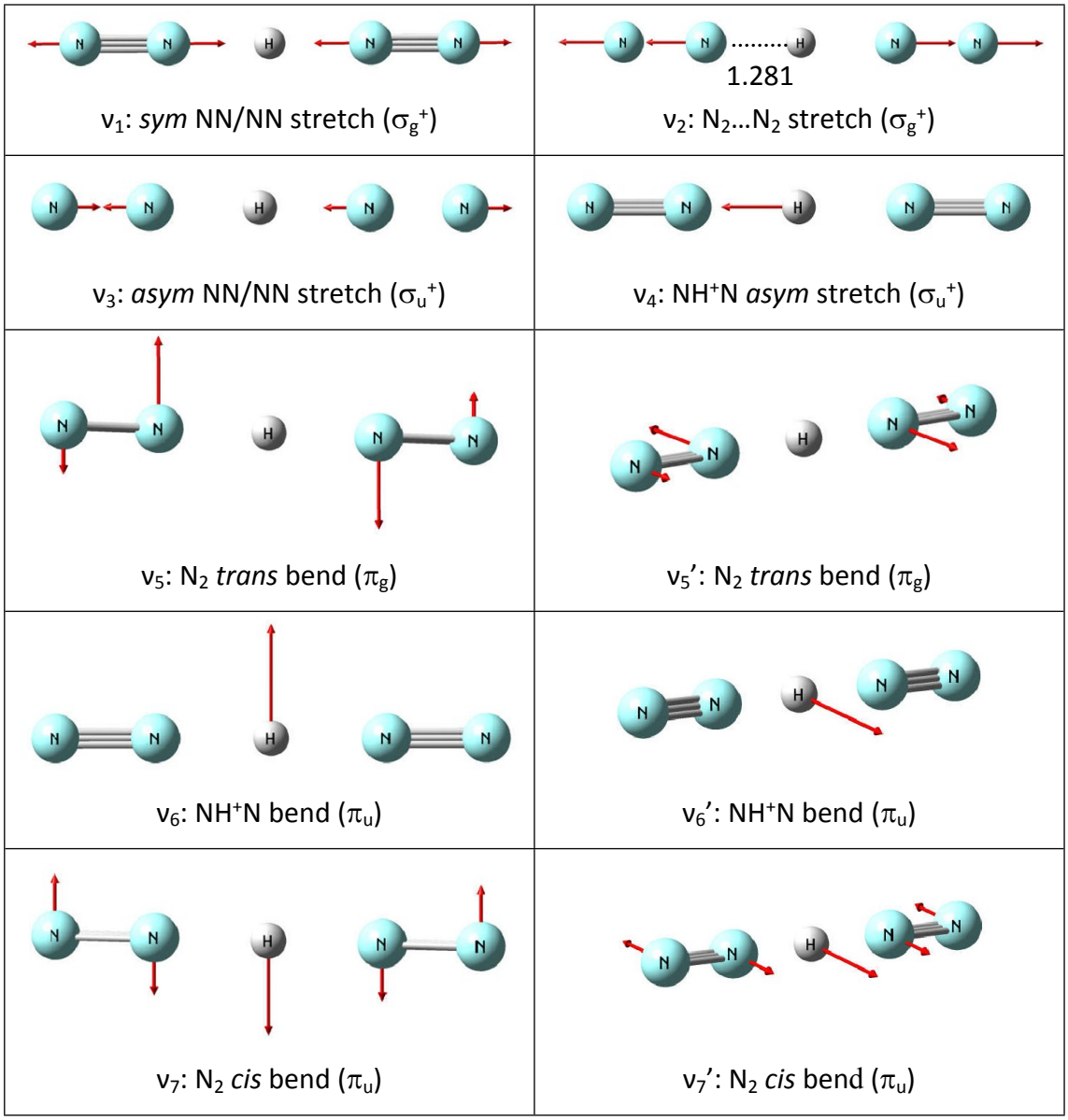

Fig. S1 Displacement vectors for normal modes of $(N_2)_2H^+$ calculated with the CCSD/aug-cc-pVDZ method. The mode numbering follows that of Duncan and coworkers.[10] Irreducible representations of modes in $D_{\infty h}$ point group are given in parentheses. Bond distances are in Å. Abbreviations *sym*, *asym*, *ip*, and *oop* represent symmetric, antisymmetric, in-plane, and out-of-plane, respectively.

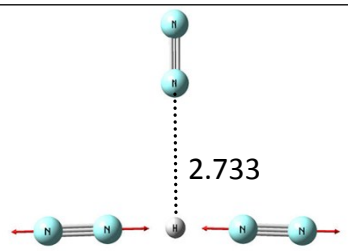 ν_1: *sym* NN/NN stretch (a_1)	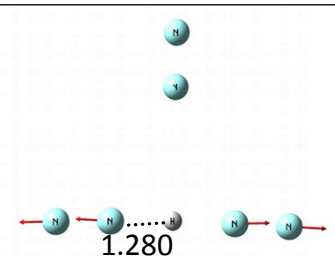 ν_2: N_2…N_2 stretch (a_1)	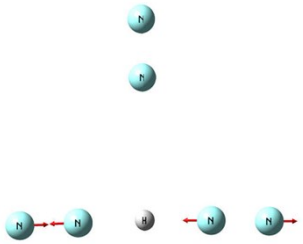 ν_3: *asym* NN/NN stretch (b_1)
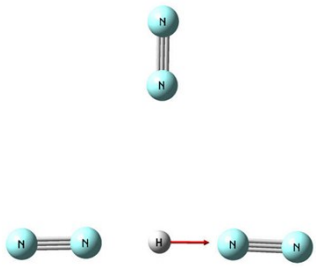 ν_4: NH^+N *asym* stretch (b_1)	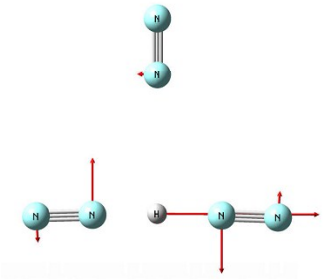 ν_5: *ip* N_2 *trans* bend /NH^+N a*sym* stretch (b_1)	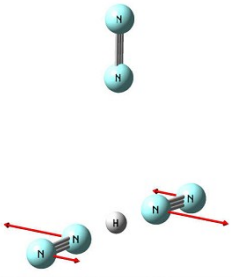 ν_5': *oop* N_2 *trans* bend (a_2)
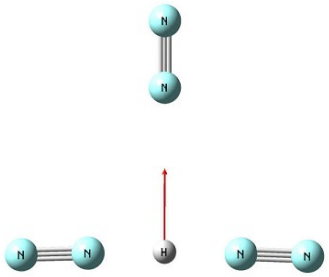 ν_6: *ip* NH^+N bend (a_1)	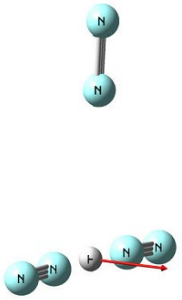 ν_6': *oop* NH^+N bend (b_2)	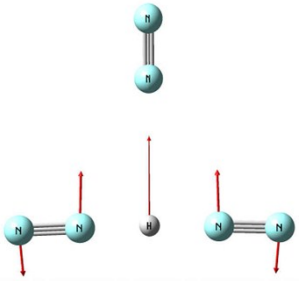 ν_7: *ip* N_2 *cis* bend (a_1)
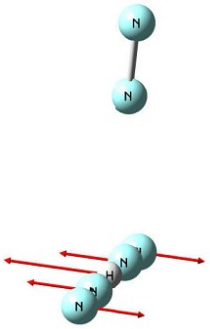 ν_7': *oop* N_2 *cis* bend (b_2)	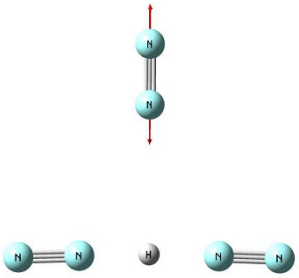 ν_8: N'N' stretch (a_1)	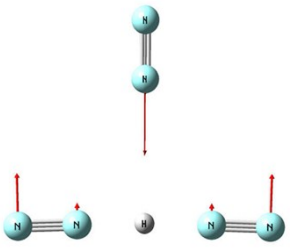 ν_9: $H^+(N'_2)$ stretch /*ip* deform (a_1)
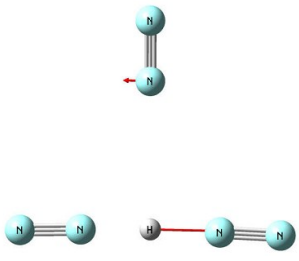 ν_{10}: *ip* N'N'H^+ bend /NH^+N *asym* stretch (b_1)	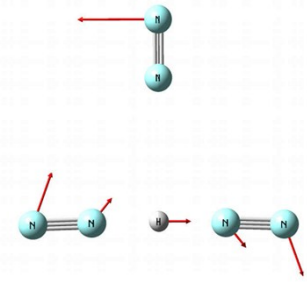 ν_{11}: *ip* deform (b_1)	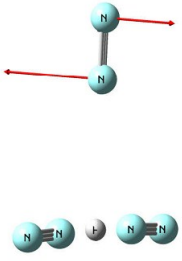 ν_{12}: *oop* deform (b_2)

Fig. S2 Displacement vectors for normal modes of $(N_2)_3H^+$ calculated with the CCSD/aug-cc-pVDZ method. For ease of comparison, we used the same vibrational mode numbers of $(N_2)_2H^+$ for the corresponding modes and listed the additional modes as ν_8–ν_{12}; when the original degeneracy in $(N_2)_2H^+$ is lifted due to the third N_2, we keep the same mode number for the in-plane mode and used a prime to indicate the second (out-of-plane) mode. Irreducible representations of modes in C_{2v} point group are given in parentheses. Bond distances are in Å. Abbreviations *sym*, *asym*, *ip*, and *oop* represent symmetric, antisymmetric, in-plane, and out-of-plane, respectively.

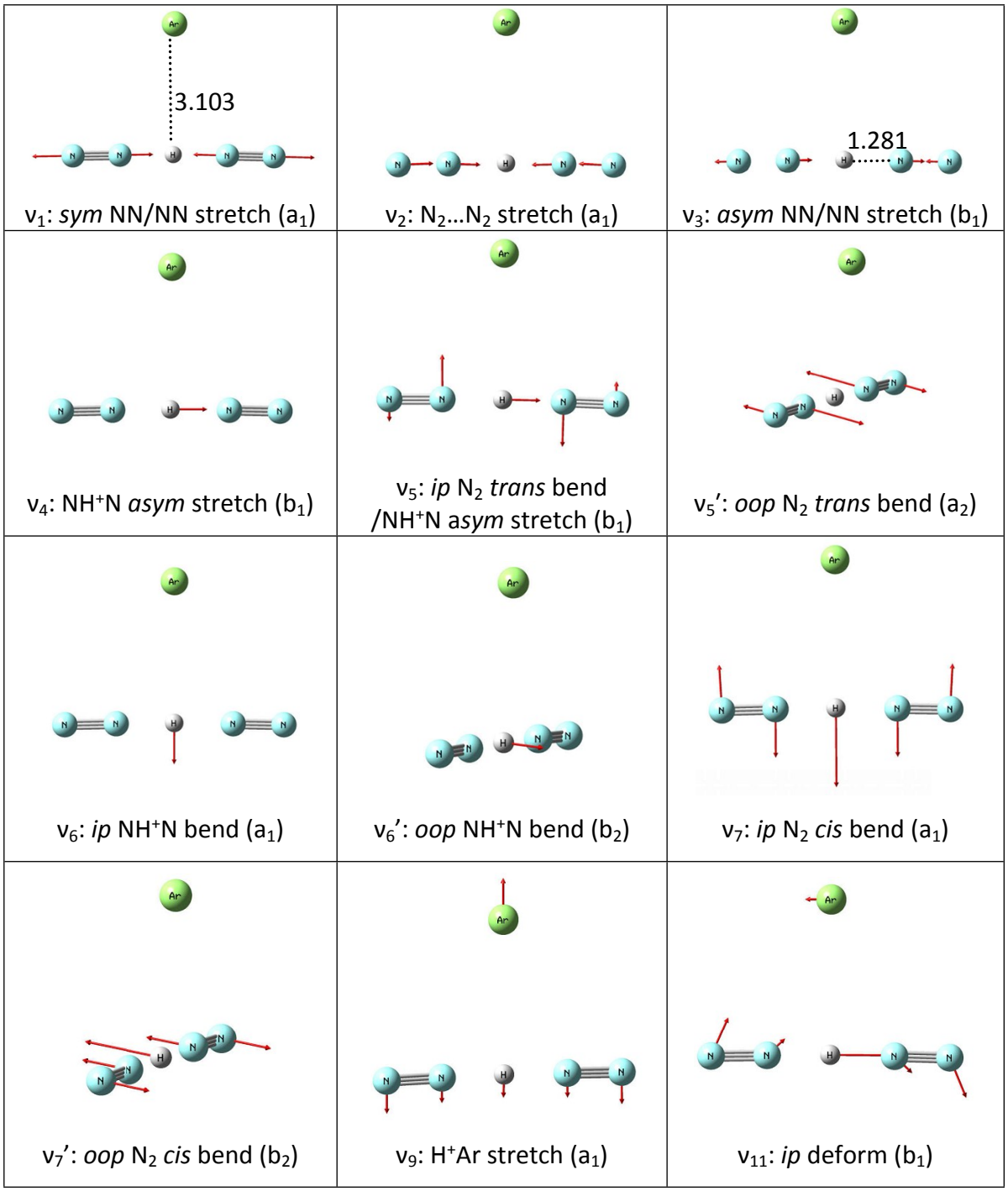

Fig. S3 Displacement vectors for normal modes of Ar-$(N_2)_2H^+$ calculated with the CCSD/aug-cc-pVDZ method. The mode numbering follows that of $(N_2)_3H^+$; the additional modes as compared with those of $(N_2)_2H^+$ are ν_9 and ν_{11}. Irreducible representations of modes in C_{2v} point group are given in parentheses. Bond distances are in Å. Abbreviations *sym*, *asym*, *ip*, and *oop* represent symmetric, antisymmetric, in-plane, and out-of-plane, respectively.

C. Examination of the number of grid points per dimension for DVR calculations

As shown in Table S2, the vibrational wavenumber of the line with the greatest intensity (ν_4) converges around grid point 11 (within 10 cm^{-1}). The vibrational wavenumber of the relatively harmonic mode ν_2 (shaded by gray) converges at grid point = 7 (within 10 cm^{-1}). We hence chose 11 and 7 as the DVR grids per degree of freedom for the anharmonic and relatively harmonic modes, respectively, in the calculations.

Table S2 Calculated two-dimensional vibrational wavenumbers (in cm^{-1}) and IR intensities (in km mol^{-1}) for coupling the $N_2…N_2$ stretching (ν_2) mode with the NH^+N antisymmetric stretching (ν_4) mode in $(N_2)_2H^+$. Calculation was performed at the CCSD/aug-cc-pVDZ level of theory with varied grid points (GPs) from 7 to 15.

Modes[a]	(sym)	GPs = 7	GPs = 9	GPs = 11	GPs = 13	GPs = 15
ν_2	(σ_g^+)	399 (0)	399 (0)	393 (0)	390 (0)	391 (0)
$2\nu_2$	(σ_g^+)	801 (0)	785 (0)	771 (0)	769 (0)	771 (0)
ν_4	(σ_u^+)	814 (3958)	891 (3668)	887 (3243)	879 (3226)	878 (3285)
$3\nu_2$	(σ_g^+)	1229 (0)	1166 (0)	1137 (0)	1135 (0)	1136 (0)
$\nu_2 + \nu_4$	(σ_u^+)	1232 (890)	1225 (1162)	1210 (1490)	1216 (1480)	1219 (1416)
$4\nu_2$	(σ_g^+)	1726 (0)	1579 (0)	1511 (0)	1494 (0)	1486 (0)
$2\nu_2 + \nu_4$	(σ_u^+)	1706 (154)	1607 (243)	1563 (366)	1558 (393)	1551 (386)
$5\nu_2$	(σ_g^+)	2321 (0)	2054 (0)	1926 (0)	1868 (0)	1833 (0)
$3\nu_2 + \nu_4$	(σ_u^+)	2290 (16)	2080 (27)	1971 (51)	1924 (71)	1889 (82)
$2\nu_4$	(σ_g^+)	2388 (0)	2254 (0)	2157 (0)	2156 (0)	2174 (0)
$6\nu_2$	(σ_g^+)	2732 (0)	2603 (0)	2400 (0)	2284 (0)	2207 (0)
$4\nu_2 + \nu_4$	(σ_u^+)	3021 (1)	2643 (2)	2448 (4)	2341 (8)	2265 (12)
$\nu_2 + 2\nu_4$	(σ_g^+)	3108 (0)	2702 (0)	2607 (0)	2584 (0)	2575 (0)
$7\nu_2$	(σ_g^+)	3138 (0)	3074 (0)	2930 (0)	2753 (0)	2626 (0)
$5\nu_2 + \nu_4$	(σ_u^+)	3668 (0)	3135 (10)	2998 (0)	2819 (1)	2693 (1)
$2\nu_2 + 2\nu_4$	(σ_g^+)	4022 (0)	3300 (0)	3066 (0)	3005 (0)	2972 (0)
$3\nu_4$	(σ_u^+)	3753 (10)	3308 (2)	3298 (18)	3273 (0)	3094 (0)
$8\nu_2$	(σ_g^+)	4281 (0)	3582 (0)	3475 (0)	3358 (0)	3175 (0)
$9\nu_2$	(σ_g^+)	4528 (0)	3835 (17)	3620 (0)	3450 (0)	3381 (0)

[a] The modes were assigned according to the results from GPs = 11.

D. Examination of the levels of theory for DVR calculations

Table S3 Comparison of calculated two-dimensional vibrational wavenumbers (in cm^{-1}) and intensities (in km mol^{-1}; listed in parentheses) of $(N_2)_2H^+$ for coupling the $N_2…N_2$ stretching (ν_2) mode with the NH^+N antisymmetric stretching (ν_4) mode with previously reported values.[a]

This work				Previous work		
CCSD/ADZ[b] 2D	CCSD/ATZ[b] 2D	CCSD(T)/ADZ[b] 2D	CCSD(T)/ATZ[b] 2D	VSCF/VCI 5MR[c]	CCSD(T)/CBS 2D[d]	CCSD(T)/cc-pVQZ 3D[e]
393 (0)	410 (0)	387 (0)	404 (0)	385.6	387 (0)	383
771 (0)	807 (0)	761 (0)	796 (0)	780.3	761 (0)	751
887 (3243)	947 (3480)	891 (3252)	950 (3473)	758.8 (2928.9)	849 (3043)	783
1137 (0)	1189 (0)	1127 (0)	1173 (0)	–	–	–
1210 (1490)	1284 (1341)	1214 (1512)	1284 (1361)	1014.1 (21.1)	1177 (1298)	–
1511 (0)	1560 (0)	1508 (0)	1544 (0)	1510.2	–	–
1563 (366)	1629 (306)	1574 (359)	1629 (312)	–	1493 (374)	–
1926 (0)	1939 (0)	1938 (0)	1931 (0)	–	–	–
1971 (51)	1999 (50)	1997 (45)	2007 (49)	–	1795 (90)	–
2157 (0)	2268 (0)	2143 (0)	2251 (0)	–	2116 (0)	–
2400 (0)	2367 (0)	2427 (0)	2363 (0)	–	–	–
2448 (4)	2415 (6)	2491 (3)	2440 (5)	–	2083 (16)	–
2607 (0)	2710 (0)	2592 (0)	2687 (0)	–	–	–
2930 (0)	2829 (0)	2965 (0)	2854 (0)	–	–	–
2998 (0)	2895 (1)	3059 (0)	2940 (0)	–	–	–
3066 (0)	3134 (0)	3074 (0)	3110 (0)	–	–	–
3298 (18)	3361 (0)	3291 (16)	3404 (0)	–	3386 (8)	–
3475 (0)	3415 (14)	3502 (0)	3405 (13)	–	–	–
3620 (0)	3445 (0)	3677 (0)	3512 (0)	–	–	–

[a] The structure was optimized at the CCSD/aug-cc-pVDZ level of theory and the number of DVR grid points per degree of freedom is eleven.
[b] ADZ denotes aug-cc-pVDZ and ATZ denotes aug-cc-pVTZ.
[c] The results are obtained from a semiglobal full-dimensional potential energy surface; see ref. 14 for more details.
[d] Infrared intensities (in km mol^{-1}) are calculated from reported transition intensities (in $Debye^2$). Frequencies are obtained from coupling ν_2 mode with ν_4 mode; see ref. 13 for more details.
[e] In addition to the ν_2 and ν_4 modes, the bending motion of the molecule is taken into account assuming $(N_2)_2H^+$ to be a pseudo-triatomic molecule; see refs. 9 and 12 for more details.

E. Comparison of vibrational wavenumbers and IR intensities of $(N_2)_2H^+$ predicted with DVR calculations of varied dimensions

Table S4 Calculated two-, three-, and four-dimensional vibrational wavenumbers (in cm^{-1}) and IR intensities (in km mol^{-1}; listed in parentheses) for coupling the N_2…N_2 stretching (ν_2) mode and the NH^+N antisymmetric stretching (ν_4) mode with the N_2 *cis* bending (ν_7), N_2 *trans* bending (ν_5), antisymmetric NN/NN stretching (ν_3), or NH^+N bending (ν_6 /$\nu_{6'}$) modes in $(N_2)_2H^+$.[a]

This work						Previous work		
2-D	3-D	3-D	3-D	3-D	4-D	VSCF/VCI	CCSD(T)/CBS	CCSD(T)/cc-pVQZ
ν_2, ν_4	ν_2, ν_4, ν_7	ν_2, ν_4, ν_5	ν_2, ν_4, ν_3	ν_2, ν_4, ν_6	ν_2, ν_4, ν_6, ν_6'	5MR[b]	2D[c]	3D[d]
–	225 (5)	–	–	–	–	146.0 (8.5)	–	–
–	–	297 (0)	–	–	–	260.4	–	–
393 (0)	393 (0)	393 (0)	390 (0)	386 (0)	378 (0)	385.6	387 (0)	383
771 (0)	772 (0)	772 (0)	767 (0)	756 (0)	739 (0)	780.3	761 (0)	751
887 (3243)	899 (3275)	896 (3268)	878 (3203)	826 (3146)	763 (3060)	758.8 (2928.9)	849 (3043)	783
–	–	–	–	–	–	1014.1 (21.1)	–	–
1210 (1490)	1222 (1475)	1219 (1480)	1199 (1460)	1145 (1512)	1080 (1519)	–	1177 (1298)	–
–	–	–	–	1147 (126)	1144 (127)	1165.8 (68.2)	–	–
–	–	–	–	–	1144 (127)	–	–	–
–	–	–	–	–	–	1329.5	–	–
1563 (366)	1572 (361)	1570 (357)	1553 (344)	1494 (378)	1426 (388)	1510.2	1493 (374)	–
1971 (51)	1973 (51)	1971 (52)	1963 (39)	1897 (52)	1824 (53)	–	1795 (90)	–
–	–	–	–	2366 (4)	2287 (4)	–	2083 (16)	–
–	–	–	2132 (0)	–	–	–	2116 (0)	–
–	–	–	–	–	–	2335, 2376	–	–
–	–	–	2425 (326)	–	–	2355.8 (213.9)	–	–
–	–	–	2444 (47)	–	–	–	–	–
–	–	–	3167 (1)	3133 (7)	3032 (7)	–	–	–
3298 (18)	3317 (17)	3312 (17)	3301 (22)	3261 (21)	3204 (32)	–	3386 (8)	–

[a] The DVR calculations were performed at the CCSD/aug-cc-pVDZ level of theory. The number of DVR grid points is 11 for ν_2 and ν_4, and 7 for other modes.

[b] The results are obtained from a semiglobal full-dimensional potential energy surface; see ref. 14 for more details.

[c] Infrared intensities (in km mol^{-1}) are calculated from reported transition intensities (in $Debye^2$). Frequencies are obtained from coupling ν_2 mode with ν_4 mode; see ref. 13 for more details.

[d] In addition to the ν_2 and ν_4 modes, the bending motion of the molecule is taken into account assuming $(N_2)_2H^+$ to be a pseudo-triatomic molecule; see refs. 9 and 12 for more details.

Table S5 Five-dimensional DVR results for combining ν_1, ν_3, ν_5, and ν_7 modes separately to the (ν_2, ν_4, ν_6, ν_6') manifold of $(N_2)_2H^+$.[a]

Modes	(Symmetry)	4-D ν_2, ν_4, ν_6, ν_6'	5-D ν_1, ν_2, ν_4, ν_6, ν_6'	5-D ν_2, ν_3, ν_4, ν_6, ν_6'	5-D ν_2, ν_4, ν_5, ν_6, ν_6'	5-D ν_2, ν_4, ν_6, ν_6', ν_7
ν_7	(π_u)	–	–	–	–	220 (5)
ν_5	(π_g)	–	–	–	289 (0)	–
ν_2	(σ_g^+)	378 (0)	375 (0)	376 (0)	378 (0)	379 (0)
ν_4	(σ_u^+)	763 (3060)	742 (2947)	754 (3033)	771 (3077)	775 (3091)
$\nu_4 + \nu_5$	(π_u)	–	–	–	1053 (31)	–
$\nu_2 + \nu_4$	(σ_u^+)	1080 (1519)	1055 (1579)	1070 (1503)	1086 (1490)	1092 (1493)
ν_6	(π_u)	1144 (127)	1142 (128)	1144 (128)	1141 (127)	1141 (127)
ν_6'	(π_u)	1144 (127)	1142 (128)	1144 (128)	1157 (98)	1142 (127)
$\nu_5 + \nu_6$	($\sigma_u^+ + \sigma_u^- + \delta_u$)	–	–	–	1468 (50)	–
$2\nu_2 + \nu_4$	(σ_u^+)	1426 (388)	1403 (422)	1417 (374)	1429 (354)	1435 (380)
$3\nu_2 + \nu_4$	(σ_u^+)	1824 (53)	1807 (57)	1818 (46)	1829 (47)	1826 (51)
ν_1	(σ_g^+)	–	2360 (0)	–	–	–
ν_3	(σ_u^+)	–	–	2423 (322)	–	–

[a] Vibrational wavenumbers (in cm^{-1}) and IR intensities (in km mol^{-1}; listed in parentheses) are shown. The DVR calculations were performed at the CCSD/aug-cc-pVDZ level of theory. The number of DVR grid points for 4-D is ($\nu_2 \times \nu_4 \times \nu_6 \times \nu_6'$) = (11 × 11 × 7 × 7) and for 5-D is ($\nu_2 \times \nu_4 \times \nu_6 \times \nu_6' \times \nu_1/\nu_3/\nu_5/\nu_7$) = (9 × 9 × 7 × 7 × 7).

F. Comparison of IR spectra of electron bombarded $N_2/p\text{-}H_2$, $^{15}N_2/p\text{-}H_2$ and $N_2/n\text{-}D_2$ matrices with varied mixing ratios

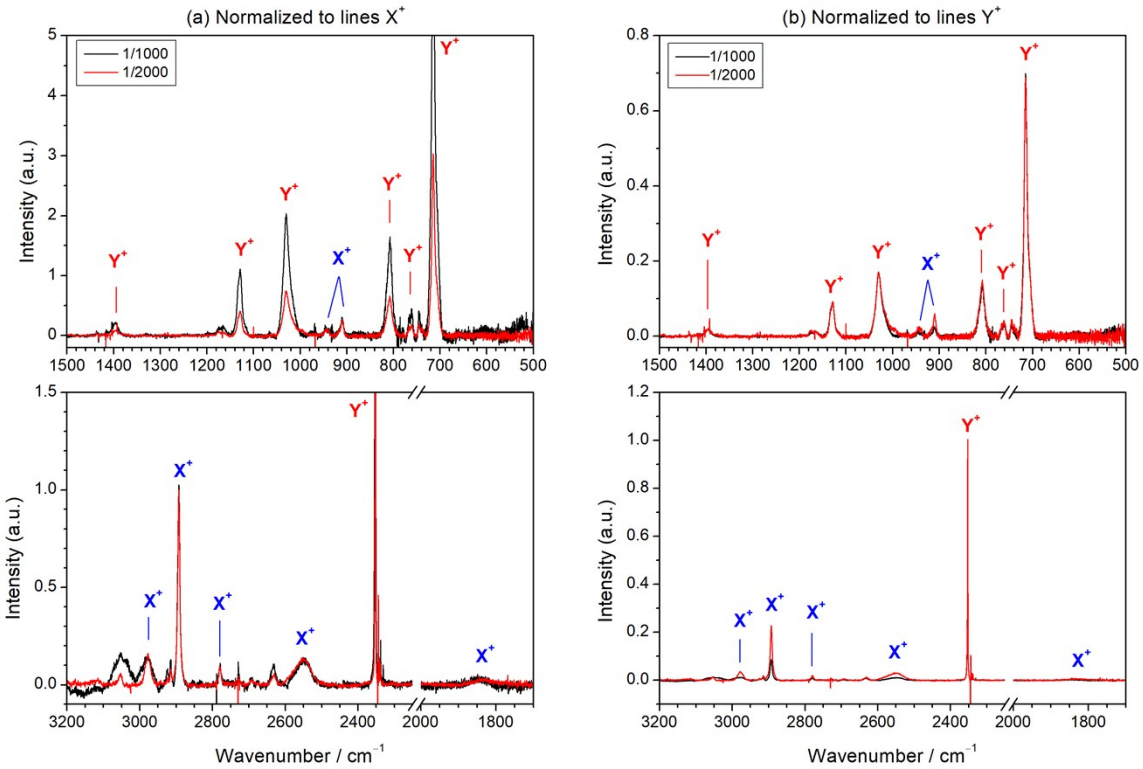

Fig. S4 Partial IR spectra of electron bombarded $N_2/p\text{-}H_2$ = 1/1000 (black trace) and 1/2000 (red trace) matrices. The spectra are inverted difference spectra showing the result of UV irradiation of deposited matrix; lines pointing upward indicate destruction. Spectra on the left column (a) were normalized with respect to the line at 2892.6 cm^{-1} (group X^+) and those on the right column (b) were normalized to the line at 2352.7 cm^{-1} (group Y).

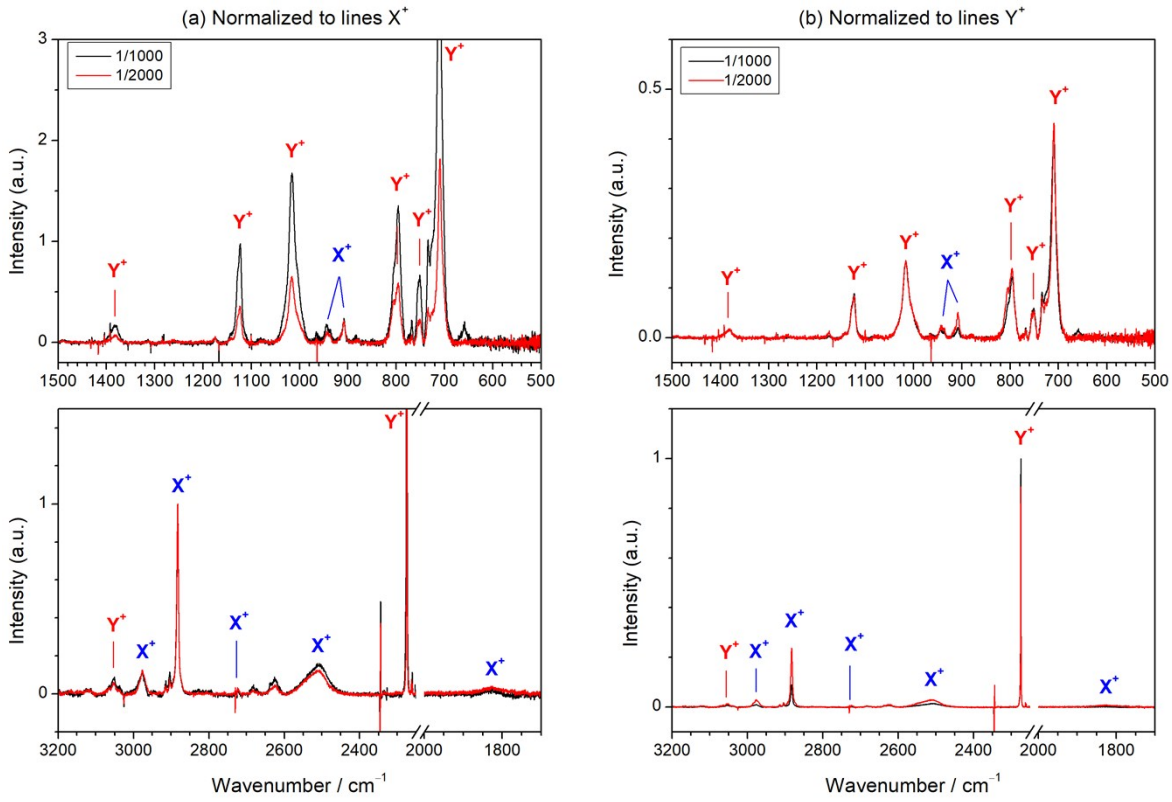

Fig. S5 Partial IR spectra of electron bombarded $^{15}N_2/p$-H_2 = 1/1000 (black trace) and 1/2000 (red trace) matrices. The spectra are inverted difference spectra showing the result of UV irradiation of deposited matrix; lines pointing upward indicate destruction. Spectra on the left column (a) were normalized with respect to the line at 2882.3 cm^{-1} (group X^+) and those on the right column (b) were normalized to the line at 2274.9 cm^{-1} (group Y^+).

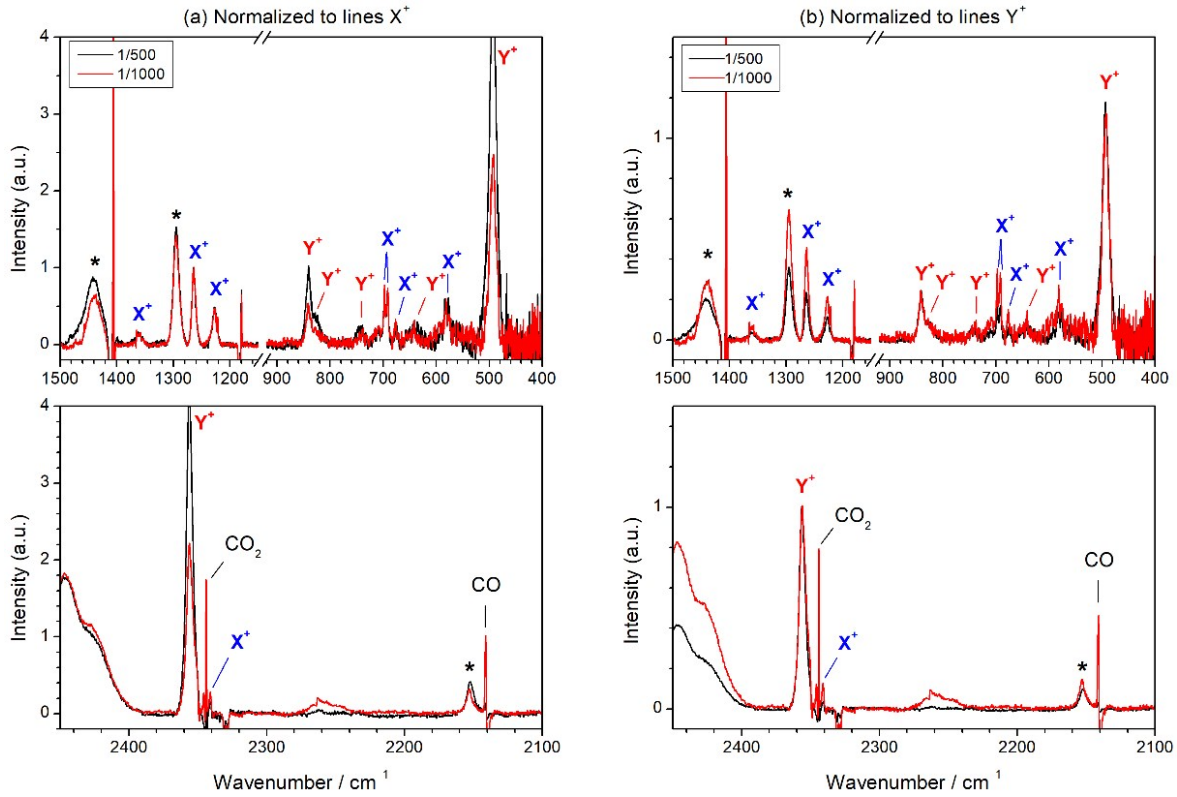

Fig. S6 Partial IR spectra of electron bombarded N_2/*n*-D_2 = 1/500 (black trace) and 1/1000 (red trace) matrices. The spectra shown are difference spectra showing the result of UV irradiation of deposited matrix. Spectra on the left column (a) were normalized with respect to the line at 1263.5 cm^{-1} (group X^+) and those on the right column (b) were normalized to the line at 2356.2 cm^{-1} (group Y^+). Lines marked with an asterisk (*) might originate from N_2D^+ perturbed by other molecule or matrix.

G. Comparison of calculated vibrational wavenumbers and IR intensities of $(N_2)_2H^+$ isotopologues

Table S6 Vibrational wavenumbers (ν), IR intensity (in km mol^{-1}; shown in parentheses), and isotopic ratios for $(^{14}N_2)_2H^+$, $(^{15}N_2)_2H^+$, and $(^{14}N_2)_2D^+$ calculated with the 4-D ($\nu_2 \times \nu_4 \times \nu_6 \times \nu_6'$) DVR calculations at the CCSD/aug-cc-pVDZ level of theory.

		$(^{14}N_2)_2H^+$	$(^{15}N_2)_2H^+$		$(^{14}N_2)_2D^+$	
Mode	(Symmetry)	ν / cm^{-1}	ν / cm^{-1}	Isotopic ratio[a]	ν / cm^{-1}	Isotopic ratio[a]
ν_2	(σ_g^+)	378 (0)	366 (0)	0.967 [–]	377 (0)	0.996 [–]
ν_4	(σ_u^+)	763 (3060)	763 (3002)	1.000 [0.993]	499 (1967)	0.654 [0.691]
$\nu_2 + \nu_4$	(σ_u^+)	1080 (1519)	1069 (1548)	0.990 [0.987]	833 (516)	0.771 [0.816]
ν_6	(π_u)	1144 (127)	1142 (128)	0.998 [0.995]	845 (56)	0.739 [0.731]
$2\nu_2 + \nu_4$	(σ_u^+)	1426 (388)	1402 (214)	0.983 [0.992]	1168 (92)	0.819 [–]
$\nu_2 + 2\nu_{10}$	(a_1)	808, 828 (61, 208) [b]	793, 803 (73, 111) [b]	0.982, 0.970 [0.986]	809 (0) [b]	1.002, 0.977 [–]
$2\nu_2 + \nu_{11}$	(b_1)	865 (276) [b]	835 (351) [b]	0.964 [0.986]	828 (95) [b]	0.956 [0.914]

[a] Isotopic ratio is defined as the ratio of wavenumber of isotopically substituted species to that of $^{14}N_2$-H^+-$^{14}N_2$. Experimental data is listed in square bracket.

[b] Obtained from protonated trimer $(N_2)_3H^+$ with the 6-D DVR method at the CCSD/aug-cc-pVDZ level of theory; see text

H. Comparison of harmonic vibrational wavenumbers and IR intensities of $(N_2)_2H^+$, $(N_2)_3H^+$ and Ar-$(N_2)_2H^+$ and their ^{15}N- and D-isotopologues

Table S7 Harmonic vibrational wavenumbers (in cm^{-1}), IR intensity (in km mol^{-1}; listed in parentheses), and approximate mode description of $(N_2)_2H^+$, $(N_2)_3H^+$, and Ar-$(N_2)_2H^+$ calculated with the CCSD/aug-cc-pVDZ method.

Mode[a]	Symmetry[b]	$(N_2)_2H^+$	$(N_2)_3H^+$	Ar-$(N_2)_2H^+$	Approximate description[c]
ν_1	σ_g^+/a_1	2458 (0)	2461 (0)	2459 (0)	*sym* NN/NN stretch
ν_2	σ_g^+/a_1	437 (0)	437 (0)	437 (0)	$N_2\ldots N_2$ stretch
ν_3	σ_u^+/b_1	2424 (264)	2426 (245)	2425 (249)	*asym* NN/NN stretch
ν_4	σ_u^+/b_1	590 (5524)	624 (2812)	603 (4822)	NH^+N *asym* stretch
ν_5	π_g/b_1	250 (0)	286 (931)	259 (109)	*ip* N_2 *trans* bend / NH^+N a*sym* stretch
ν_5'	π_g/a_2	250 (0)	250 (0)	250 (0)	*oop* N_2 *trans* bend
ν_6	π_u/a_1	1217 (90)	1188 (121)	1197 (114)	*ip* NH^+N bend
ν_6'	π_u/b_2	1217 (90)	1224 (80)	1222 (80)	*oop* NH^+N bend
ν_7	π_u/a_1	141 (6)	153 (13)	146 (10)	*ip* N_2 *cis* bend
ν_7'	π_u/b_2	141 (6)	143 (6)	142 (6)	*oop* N_2 *cis* bend
ν_8	$-/a_1$	–	2397 (7)	–	N'N' stretch
ν_9	$-/a_1$	–	83 (5)	60 (8)	H^+Ar stretch[d]
ν_{10}	$-/b_1$	–	179 (1416)	–	*ip* $N'N'H^+$ bend / NH^+N *asym* stretch
ν_{11}	$-/b_1$	–	48 (10)	55 (214)	*ip* deform
ν_{12}	$-/b_2$	–	95 (0)	–	*oop* deform

[a] For ease of comparison, we employed the same mode numbering of $(N_2)_2H^+$ for modes ν_1–ν_7 of $(N_2)_3H^+$ and Ar-$(N_2)_2H^+$, and add the additional modes as ν_8–ν_{12} for $(N_2)_3H^+$ and ν_9 and Ar-$(N_2)_2H^+$.
[b] The symmetry group is $D_{\infty h}$ for $(N_2)_2H^+$ and C_{2v} for $(N_2)_3H^+$ and Ar-$(N_2)_2H^+$.
[c] *sym*: symmetric; *asym*: antisymmetric; *ip*: in-plane; *oop*: out-of-plane. The N atoms in the third N_2 are indicated as N'.
[d] For $(N_2)_3H^+$ this mode is $H^+(N'_2)$ stretch mixed with *ip* deform.

Table S8 Harmonic vibrational wavenumbers (in cm^{-1}), IR intensity (in km mol^{-1}; listed in parenthesis), and approximate mode description of $(N_2)_2D^+$, $(N_2)_3D^+$, and Ar-$(N_2)_2D^+$ calculated with the CCSD/aug-cc-pVDZ method.

Mode[a]	Symmetry[b]	$(N_2)_2D^+$	$(N_2)_3D^+$	Ar-$(N_2)_2D^+$	Approximate description[c]
ν_1	σ_g^+/a_1	2458 (0)	2460 (0)	2459 (0)	*sym* NN/NN stretch
ν_2	σ_g^+/a_1	437 (0)	437 (0)	437 (0)	$N_2 \ldots N_2$ stretch
ν_3	σ_u^+/b_1	2423 (233)	2426 (215)	2424 (220)	*asym* NN/NN stretch
ν_4	σ_u^+/b_1	434 (2774)	448 (1521)	427 (2331)	ND^+N *asym* stretch
ν_5	π_g/b_1	250 (0)	274 (243)	257 (43)	*ip* N_2 *trans* bend / ND^+N a*sym* stretch
ν_5'	π_g/a_2	250 (0)	250 (0)	250 (0)	*oop* N_2 *trans* bend
ν_6	π_u/a_1	887 (39)	867 (52)	872 (49)	*ip* ND^+N bend
ν_6'	π_u/b_2	887 (39)	891 (34)	890 (34)	*oop* ND^+N bend
ν_7	π_u/a_1	139 (5)	149 (12)	143 (9)	*ip* N_2 *cis* bend
ν_7'	π_u/b_2	139 (5)	140 (5)	139 (5)	*oop* N_2 *cis* bend
ν_8	$-/a_1$	–	2397 (7)	–	N'N' stretch
ν_9	$-/a_1$	–	83 (5)	60 (8)	D^+Ar stretch[d]
ν_{10}	$-/b_1$	–	161 (823)	–	*ip* $N'N'D^+$ bend / ND^+N *asym* stretch
ν_{11}	$-/b_1$	–	48 (10)	55 (210)	*ip* deform
ν_{12}	$-/b_2$	–	95 (0)	–	*oop* deform

[a] For ease of comparison, we employed the same mode numbering of $(N_2)_2D^+$ for modes ν_1–ν_7 of $(N_2)_3D^+$ and Ar-$(N_2)_2D^+$, and add the additional modes as ν_8–ν_{12} for $(N_2)_3H^+$ and ν_9 and Ar-$(N_2)_2H^+$.

[b] The symmetry group is $D_{\infty h}$ for $(N_2)_2D^+$ and C_{2v} for $(N_2)_3D^+$ and Ar-$(N_2)_2D^+$.

[c] *sym*: symmetric; *asym*: antisymmetric; *ip*: in-plane; *oop*: out-of-plane. The N atoms in the third N_2 are indicated as N'.

[d] For $(N_2)_3D^+$ this mode is $D^+(N'_2)$ stretch mixed with *ip* deform.

Table S9 Harmonic vibrational wavenumbers (in cm^{-1}), IR intensity (in km mol^{-1}; listed in parentheses), and approximate mode description of $(^{15}N_2)_2H^+$, $(^{15}N_2)_3H^+$, and Ar-$(^{15}N_2)_2H^+$ calculated with the CCSD/aug-cc-pVDZ method.

Mode[a]	Symmetry[b]	$(^{15}N_2)_2H^+$	$(^{15}N_2)_3H^+$	Ar-$(^{15}N_2)_2H^+$	Approximate description[c]
ν_1	σ_g^+/a_1	2375 (0)	2377 (0)	2376 (0)	*sym* $^{15}N^{15}N/^{15}N^{15}N$ stretch
ν_2	σ_g^+/a_1	422 (0)	423 (0)	422 (0)	$^{15}N_2\ldots{}^{15}N_2$ stretch
ν_3	σ_u^+/b_1	2342 (251)	2344 (232)	2343 (237)	*asym* $^{15}N^{15}N/^{15}N^{15}N$ stretch
ν_4	σ_u^+/b_1	590 (5210)	623 (2794)	598 (4753)	$^{15}NH^{+15}N$ *asym* stretch
ν_5	π_g/b_1	242 (0)	278 (986)	251 (127)	*ip* $^{15}N_2$ *trans* bend / $^{15}NH^{+15}N$ a*sym* stretch
ν_5'	π_g/a_2	242 (0)	241 (0)	242 (0)	*oop* $^{15}N_2$ *trans* bend
ν_6	π_u/a_1	1215 (91)	1186 (122)	1194 (115)	*ip* $^{15}NH^{+15}N$ bend
ν_6'	π_u/b_2	1215 (91)	1221 (81)	1220 (81)	*oop* $^{15}NH^{+15}N$ bend
ν_7	π_u/a_1	137 (6)	148 (12)	141 (9)	*ip* $^{15}N_2$ *cis* bend
ν_7'	π_u/b_2	137 (6)	139 (6)	138 (5)	*oop* $^{15}N_2$ *cis* bend
ν_8	$-/a_1$	–	2316 (6)	–	$^{15}N'^{15}N'$ stretch
ν_9	$-/a_1$	–	80 (4)	59 (7)	H^+Ar stretch[d]
ν_{10}	$-/b_1$	–	174 (1379)	–	*ip* $^{15}N'^{15}N'H^+$ bend / $^{15}NH^{+15}N$ *asym* stretch
ν_{11}	$-/b_1$	–	46 (10)	55 (263)	*ip* deform
ν_{12}	$-/b_2$	–	91 (0)	–	*oop* deform

[a] For ease of comparison, we employed the same mode numbering of $(^{15}N_2)_2H^+$ for modes ν_1–ν_7 of $(^{15}N_2)_3H^+$ and Ar-$(^{15}N_2)_2H^+$, and add the additional modes as ν_8–ν_{12} for $(^{15}N_2)_3H^+$ and ν_9 and Ar-$(^{15}N_2)_2H^+$.

[b] The symmetry group is $D_{\infty h}$ for $(^{15}N_2)_2H^+$ and C_{2v} for $(^{15}N_2)_3H^+$ and Ar-$(^{15}N_2)_2H^+$.

[c] *sym*: symmetric; *asym*: antisymmetric; *ip*: in-plane; *oop*: out-of-plane. The N atoms in the third $^{15}N_2$ are indicated as $^{15}N'$.

[d] For $(^{15}N_2)_3H^+$ this mode is $H^+(^{15}N'_2)$ stretch mixed with *ip* deform.

I. Comparison of vibrational wavenumbers and IR intensities of $(N_2)_3H^+$ and Ar-$(N_2)_2H^+$ calculated with DVR calculations of varied dimensions

Table S10 Vibrational wavenumbers (in cm^{-1}) and IR intensity (in km mol^{-1}; listed in parentheses) of $(N_2)_3H^+$ calculated with five- and six-dimensional DVR.[a]

Modes	4-D ν_2, ν_4, ν_6, ν_6'	5-D ν_2, ν_4, ν_5, ν_6, ν_6'	5-D ν_2, ν_4, ν_6, ν_6', ν_9	5-D ν_2, ν_4, ν_6, ν_6', ν_{10}	5-D ν_2, ν_4, ν_6, ν_6', ν_{11}	6-D ν_2, ν_4, ν_5, ν_9, ν_{10}, ν_{11}	6-D ν_2, ν_4, ν_6, ν_6', ν_{10}, ν_{11}	6-D ν_2, ν_4, ν_7, ν_7', ν_{10}, ν_{11}
ν_{11}	–	–	–	–	93 (0)	63 (0)	67 (1)	102 (0)
ν_9	–	–	85 (5)	–	–	91 (4)	–	–
ν_{10}	–	–	–	207 (1)	–	231 (1)	226 (4)	229 (1)
ν_7'	–	–	–	–	–	–	–	239 (5)
ν_7	–	–	–	–	–	–	–	251 (11)
ν_5	–	250 (32)	–	–	–	308 (3)	–	–
ν_2	371 (0)	375 (0)	370 (0)	375 (0)	371 (0)	393 (0)	372 (0)	390 (0)
$\nu_2 + \nu_{11}$	–	–	–	–	459 (275)	–	431 (55)	483 (16)
$\nu_2 + \nu_9$	–	–	457 (0)	–	–	480 (0)	–	–
$2\nu_7' + \nu_{11}$	–	–	–	–	–	–	–	581 (0)
$\nu_2 + \nu_{10}$	–	–	–	567 (198)	–	–	594 (65)	605 (47)
$\nu_2 + \nu_5$	–	586 (1055)	–	–	–	–	–	–
$\nu_5 + 2\nu_{10} + \nu_{11}$	–	–	–	–	–	805 (36)	–	–
$\nu_2 + 2\nu_9 + \nu_{10}$	–	–	–	–	–	807 (26)	–	–
$\nu_2 + \nu_5 + 2\nu_{11}$	–	–	–	–	–	811 (24)	–	–
$2\nu_2 + \nu_{11}$	–	–	–	–	–	836 (111)	775 (14)	–
$2\nu_7 + \nu_{10}$	–	–	–	–	–	–	–	729 (48)
$2\nu_5 + \nu_{10}$	–	–	–	–	–	854 (24)	–	–
$\nu_5 + \nu_9 + 2\nu_{10}$	–	–	–	–	–	882 (228)	–	–
ν_4	490 (1915)	668 (1347)	491 (1920)	665 (2378)	506 (445), 509 (1209)	885 (2299)	663 (2150)	776 (1947)
$\nu_2 + \nu_5 + 2\nu_9$	–	–	–	–	–	901 (36)	–	–
$2\nu_2 + \nu_5$	–	936 (509)	–	–	–	–	–	–

$\nu_2 + 2\nu_{10}$	–	–	–	–	–	–	837 (0)	808 (61), 828 (208)
$2\nu_2 + \nu_{11}$	–	–	–	–	806 (199)	–	810 (38)	865 (276)
$2\nu_2 + \nu_9$	–	–	807 (0)	–	–	877 (0)	–	–
$\nu_4 + 2\nu_{11}$	–	–	–	–	–	–	820 (82)	890 (53)
$2\nu_2 + \nu_{10}$	–	–	–	926 (192)	–	1000 (68)	942 (192)	985 (111)
$\nu_2 + 2\nu_7 + \nu_{10}$	–	–	–	–	–	–	–	1109 (53)
$2\nu_7 + 2\nu_7' + \nu_{11}$	–	–	–	–	–	–	–	1116 (26)
$\nu_2 + 2\nu_5 + \nu_{10}$	–	–	–	–	–	1233 (111)	–	–
$\nu_2 + \nu_4$	813 (512)	1034 (325)	830 (543)	1024 (885)	855 (337)	1254 (223)	1011 (447)	1125 (346)
ν_6	1138 (113)	1115 (144)	1113 (170)	1106 (162)	1114 (170)	–	1107 (163)	–
ν_6'	1158 (113)	1152 (113)	1157 (103)	1152 (114)	1158 (113)	–	1150 (113)	–
$2\nu_2 + \nu_{10} + 2\nu_{11}$	–	–	–	–	–	–	1108 (53)	1208 (164)
$2\nu_2 + \nu_{10} + 3\nu_{11}$	–	–	–	–	–	–	–	1270 (74)
$2\nu_2 + \nu_4$	1113 (171)	1452 (49)	1189 (103)	1454 (138)	1158 (35), 1214 (60)	1690 (31)	1427 (55)	1525 (39)

[a] Vibrational wavenumbers (in cm^{-1}) and IR intensities (in km mol^{-1}; listed in parentheses) are shown. The DVR calculations were performed at the CCSD/aug-cc-pVDZ level of theory. The number of DVR grid points for 5-D calculation is 7 per degree of freedom and that for 6-D is (7 × 7 × 5 × 5 × 5 × 5).

Table S11 Vibrational wavenumbers (ν), IR intensity (in km mol^{-1}; listed in parentheses), and isotopic ratios for Ar-$(N_2)_2H^+$ and Ar-$(N_2)_2D^+$ predicted with varied DVR calculations. [a]

Modes	4-D: ν_2, ν_4, ν_6, ν_6'	5-D: ν_2, ν_4, ν_6, ν_6', ν_{11}			Experiments (Ref. 10)		
	Ar-$(N_2)_2H^+$	Ar-$(N_2)_2H^+$	Ar-$(N_2)_2D^+$		Ar-$(N_2)_2H^+$	Ar-$(N_2)_2D^+$	
	ν / cm^{-1}	ν / cm^{-1}	ν / cm^{-1}	Isotopic Ratio[b]	ν / cm^{-1}	ν / cm^{-1}	Isotopic Ratio[b]
ν_{11}	–	50 (1)	50 (1)	0.982	–	–	–
ν_7'	–	–	–	–	–	–	–
ν_7	–	–	–	–	–	–	–
ν_2	376 (0)	379 (0)	378 (0)	0.997	–	–	–
ν_4	698 (2638)	746 (2814)	497 (1803)	0.666	743	–	–
$2\nu_2 + \nu_{11}$	–	790 (69)	806 (18)	1.020	780	–	–
$\nu_4 + 2\nu_{11}$	–	–	–	–	983	–	–
$3\nu_2 + \nu_{11}$	–	–	–	–	–	–	–
$\nu_2 + \nu_4$	1024 (1167)	1083 (1248)	831 (397)	0.767	1051	817	0.777
ν_6	1125 (160)	1123 (159)	832 (70)	0.740	1144	853	0.746
ν_6'	1149 (114)	1146 (114)	847 (50)	0.739	–	–	–
–	–	–	–	–	1205	967	0.802
–	–	–	–	–	1300	–	–
–	–	–	–	–	1340	–	–
–	–	–	–	–	1357	1068	0.787
$2\nu_2 + \nu_4$	1369 (286)	1466 (288)	1186 (64)	0.809	1409	1129	0.801
$3\nu_2 + \nu_4$	1761 (39)	1919 (32)	1594 (5)	0.831	–	–	–

[a] The DVR calculations were performed at the CCSD/aug-cc-pVDZ level of theory. The number of DVR grid points for 5-D is ($\nu_2 \times \nu_4 \times \nu_6 \times \nu_6' \times \nu_{11}$) = ($9 \times 9 \times 7 \times 7 \times 7$).

[b] Isotopic ratio is defined as the ratio of wavenumber of isotopically substituted species to that of Ar-$(^{14}N_2)_2H^+$.

J. Potential Slice along NH^+N antisymmetric stretch

Fig. S7 shows the rigid scan on the $N{-}H^+$ bond using the minimum and transition state structure. It is anticipated that a rigid scan using the minimum geometry overestimates the barrier, whereas that using the transition state geometry underestimates the barrier. The one-dimensional slice along Q_4 is shown in Fig. S8. Due to the spacing of our quadrature grids, the ν_4 potential slice is effectively a symmetric single well.

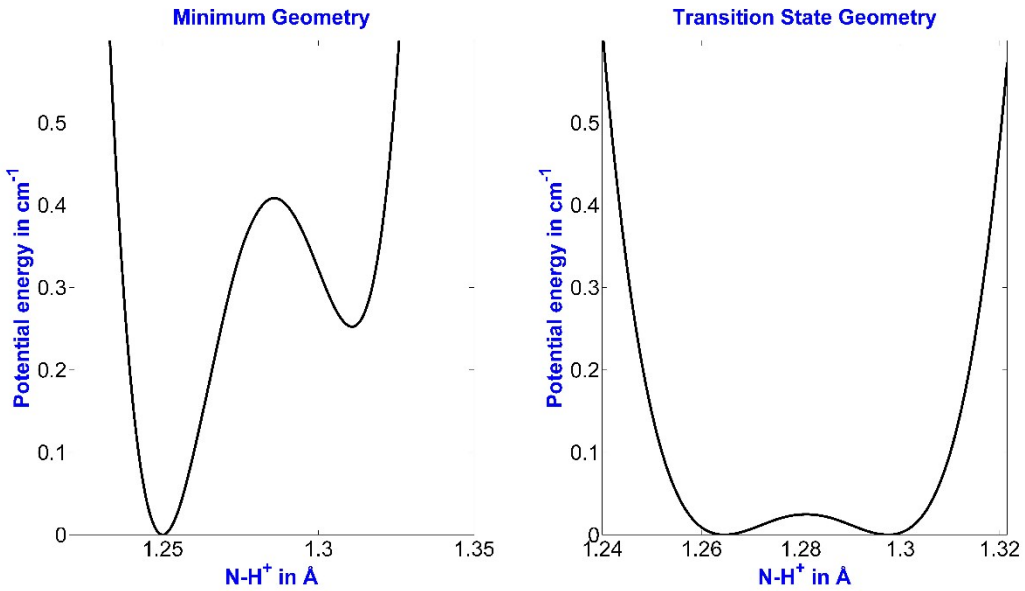

Fig. S7 Rigid $N{-}H^+$ scan using the N_2-H^+-N_2 minimum geometry (left) and transition state geometry (right). In both cases, the difference between the global minimum and the transition state is less than 0.5 cm^{-1}.

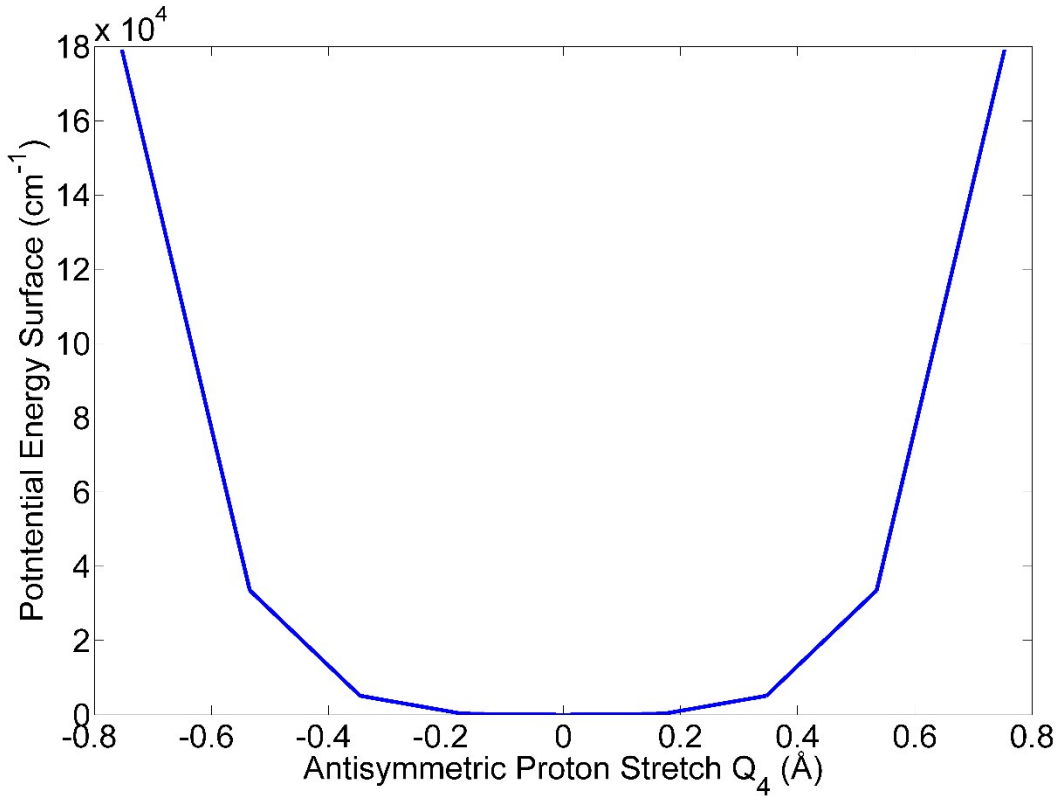

Fig. S8 The one-dimensional slice along Q_4. Due to the spacing of our quadrature grids, the potential slice is effectively a symmetric single well.